



# Radiology findings of Down syndrome: a literature review

Jacobus Jenő Wibisono<sup>1</sup> · Carissa Faustina<sup>1</sup> · Maria Georgina Wibisono<sup>1</sup> · Jeanne Leman<sup>1</sup> · Ratna Sutanto<sup>1</sup>

Received: 27 August 2023 / Revised: 18 November 2023 / Accepted: 21 November 2023 / Published online: 21 December 2023

© The Author(s), under exclusive licence to Springer Nature Singapore Pte Ltd. 2023

## Abstract

Trisomy 21, commonly known as Down syndrome (DS), stands as the most prevalent genetic source of intellectual disability worldwide. Individuals with Down syndrome may experience a range of abnormalities affecting multiple organ systems. The distinctive facial features and musculoskeletal characteristics evident at birth often make the diagnosis apparent if it has not been established during pregnancy. Depending on the severity of specific findings, children with Down syndrome may undergo radiological assessments at various stages of their development. The cardiovascular system, the digestive system, the facial look, the morphology of hearing aids, and the central nervous system can all be impacted by Down syndrome. An early diagnosis, especially during prenatal care, allows for better planning and preparation for the child's birth. Therefore, it is essential to have a comprehensive understanding of the radiological characteristics associated with Down syndrome patients. In conclusion, Down syndrome is associated with various radiological features. Indicators of Down syndrome can include the presence of atrioventricular septal abnormalities, tetralogy of Fallot, macroglossia, esophageal atresia, microcephaly, and structural alterations in the musculoskeletal system. During fetal imaging, it is important to assess the volume of amniotic fluid, particularly in the context of nuchal translucency, as well as determine the presence or absence of nasal bones in the fetus.

**Keywords** Down syndrome · Radiology findings · Nuchal translucency · Nasal bones · Fetus radiology

## Abbreviations

DS	Down syndrome	PT	Prenasal thickness
CNS	Central nervous system	OCT	Optical coherence tomography
BPD	Biparietal diameter	CST	Central subfield thickness
OFD	Occipitofrontal diameter	LSCC	Lateral semi-circular canal
CT	Computed tomography	AVSD	Atrio ventricular septal defect
MRI	Magnetic resonance imaging	RSV	Respiratory syncytial virus
NB	Nasal bone	FIESTA	Fast imaging exploiting steady-state acquisition
NBL	Nasal bone length	NT	Nuchal translucency

✉ Jacobus Jenő Wibisono  
jj\_wibisono@yahoo.co.id

Carissa Faustina  
faustinacarissa@gmail.com

Maria Georgina Wibisono  
georginaw0411@gmail.com

Jeanne Leman  
lemanjeanne@gmail.com

Ratna Sutanto  
ratnasutanto.raduph@gmail.com

<sup>1</sup> Pelita Harapan University, Jl. Jend. Sudirman No.20, Bencong, Kec. Kl. Dua, Kabupaten Tangerang, Banten 15810, Indonesia

## Background

Down syndrome, often referred to as DS, is a genetic condition characterized by the presence of an extra or partial 21 chromosome, resulting in distinct physical and intellectual characteristics [1]. Normally, humans have 46 chromosomes, with 23 inherited from each parent, but in some cases, there may be 47 chromosomes in each cell, leading to the condition known as Down syndrome. This condition was first described by the British physician John Langdon Down in 1866, hence the name [2].

The World Health Organization reports that DS occurs in approximately 1 in 1000–1100 live births. The incidence

of DS pregnancies in Europe has increased by 10% over the past two decades, possibly due to older maternal age at conception [3].

Trisomy, the genetic imbalance underlying DS, disrupts crucial developmental pathways. Trisomy induces formation, growth, or fusion of the facial prominences errors during embryonal craniofacial development, leading to orofacial deformities [1].

At birth, individuals with DS often exhibit physical features such as brachycephalic head shape, an epicanthic fold, a tiny and flat nose bridge, clinodactyly, single palmar crease, and enhanced nuchal skin. Additionally, DS is frequently associated with language, cognitive, learning, and memory deficits. Every organ system, including the spine, head, neck, and central nervous system, can be affected by DS [3].

Previous research has shown that individuals with Down syndrome have smaller dimensions in the atlantoaxial, craniovertebral, and cephalometric regions compared to those without the syndrome. These measures appear to be poorly integrated in individuals with Down syndrome, suggesting that the condition's phenotype is a result of genetic abnormalities [1]. It is important to note that Down syndrome can be diagnosed during pregnancy, emphasizing the importance of understanding the radiological characteristics of individuals with this condition.

## Radiology findings

### Prenatal

#### Nose

A significant indicator for Down syndrome is the absence of the nasal bone, which increases the likelihood of Down syndrome by a factor ranging from 20 to 60. Another critical indicator is the ratio of the length of the humerus to the average humerus length. If this ratio falls well below the expected range, the risk is elevated by a factor of 6. The ratio of biparietal diameter to nasal bone length, taking into account the gestational week, is typically  $8.1 \pm 1.4$ ; while in fetuses with trisomy 21 (Down syndrome), it measures  $11.3 \pm 2.0$ . This marker is also referred to as the frontonasal fold thickness to nasal bone length ratio. Accurate identification of these indicators is crucial, but it can be challenging due to the potential interference of ultrasound markers with underlying structures, often caused by speckle noise. Therefore, the precise recognition of these indicators requires the expertise of trained sonographers, obstetricians, and fetal medicine professionals [2].

A non-invasive procedure known as fetal nasal bone (NB) assessment offers first-trimester patients more certainty in determining the potential risk of Down syndrome in their

unborn child. This assessment involves evaluating the presence or absence of the fetal nasal bone during the first trimester of pregnancy, with the absence of the nasal bone indicating a positive test result for Down syndrome (Fig. 1) [4].

The fetal nose was gently tilted from side to side, with the ultrasound transducer positioned in alignment with the nose's direction. When these conditions were met, three distinct lines could be discerned at the level of the fetal nose. The first two lines, situated near the forehead, ran parallel to each other and were horizontal, resembling an "equals sign." The lower line, thicker and displaying more echogenic properties than the skin above it, indicated the presence of the nasal bone. The upper line represented the skin. A third line, nearly in line with the skin but slightly elevated, marked the tip of the nose. Once the nasal bone (NB) had become clearly visible, the bony portion of the nasal bridge was measured using calipers in the out-to-out position, with measurements made in 0.1 mm increments [4].

The presence of the nasal bone is determined by whether it exhibits higher echogenicity compared to the skin above it. In the first trimester, the Fetal Medicine Foundation's guidelines were employed to identify instances of a missing fetal nasal bone. In cases where the nasal bone's echogenicity did not surpass that of the overlying skin, it was considered as a sign of a missing nasal bone. When the nasal bone was entirely absent or appeared unusually small, it was deemed hypoplastic [4].

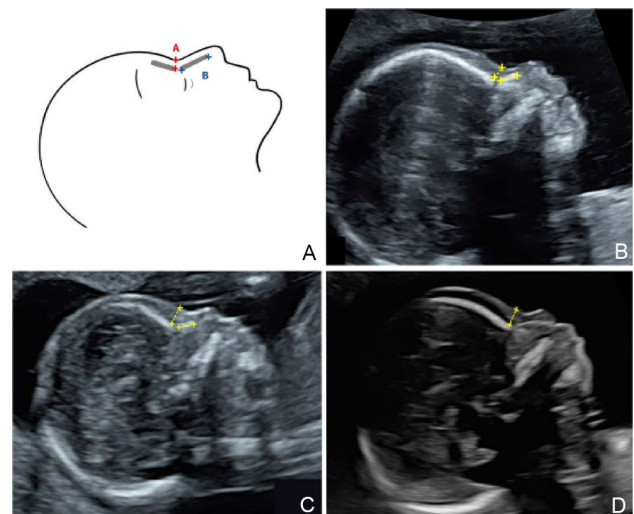


**Fig. 1** Nasal bone in DS. The landmarks for measuring the facial ultrasonography markers are depicted in (A). NBL is determined by measuring along the ossification line of the fetal nose. PT is the measurement taken from the edge of the lowest part of the frontal bone to the anterior skin of the face (A). A euploid fetus (B) and a normal fetus (A) with mid-facial ultrasound images are also displayed. Hypoplastic and missing nasal bones in a fetus with Down syndrome (C and D, respectively). NBL nasal bone length, PT prenasal thickness [5]

### Nuchal translucency

The assessment and severity evaluation of Down syndrome during pregnancy can be conducted using antenatal imaging techniques such as fetal sonography and fetal MR imaging. In the field of obstetrics and gynecology, two-dimensional ultrasound imaging is more commonly employed due to its non-invasive, cost-effective, straightforward, and safe nature. However, ultrasound imaging has limitations related to image quality. This is because the raw radio frequency signal has to undergo multiple processing steps before it can be transformed into an image, and the presence of multiplicative speckle noise can reduce image clarity. Consequently, due to the low quality of the image, it may not provide sufficient information for a healthcare provider to make an accurate diagnosis [2].

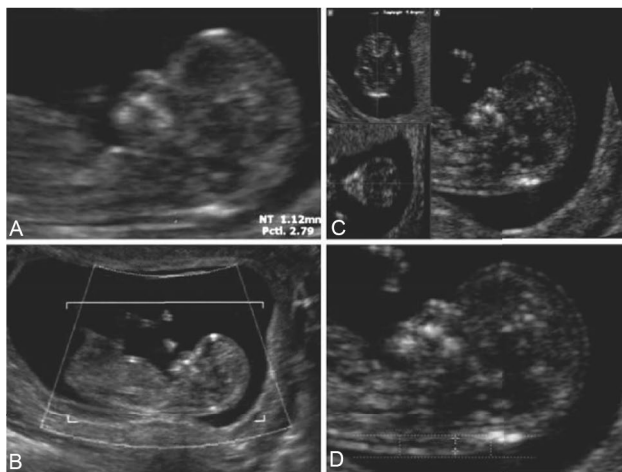


Fig. 2 The conventional 2D NT measurement

Nuchal translucency refers to the accumulation of fluid beneath the skin of the fetal neck between the 11.3 and 13.6 weeks of gestation. Babies with Down syndrome tend to have higher levels of this fluid. During this 10–13-week period, a nuchal translucency thickness of 2.2 mm–2.8 mm is considered within the normal range. An increased thickness of translucency is associated with an elevated risk. Researchers have employed blob analysis to accurately measure the thickness of the nuchal translucency region. According to their findings, by the 14th week of gestation, a typical fetus should have a nuchal translucency thickness of 1.85 mm [2].

The Fetal Medicine Foundation recommends a conventional 2D test for measuring NT, as depicted in Fig. 2. In the Volume NT approach, a 3D volume box is used to encompass the fetal head and thorax (a). By placing a caliper in the diencephalon, the system is activated, automatically capturing the appropriate mid-sagittal plane (c). The area of interest is enclosed by an adjustable frame, and the maximum vertical distance (NT) is measured at the point within the box exhibiting the highest echogenicity (d) [6].

Research has established a connection between an elevated fetal NT thickness exceeding 3 mm and an increased risk of developing Down syndrome. To measure the widest part of the translucency, the mid-sagittal plane is employed for NT calibration. Clinicians manually calculate NT using an electronic caliper, and the precision of this measurement is contingent on the operator's skill. Due to the relatively small size of NT, even a minor estimation error can lead to inaccuracies in fetal growth assessment. Consequently, computerized methods are recommended to overcome the limitations associated with manual measurements and enhance the detection rate (Fig. 3) [7].

R. Sonia and V. Shanthi propose the utilization of a computer-based approach for nuchal translucency thickness

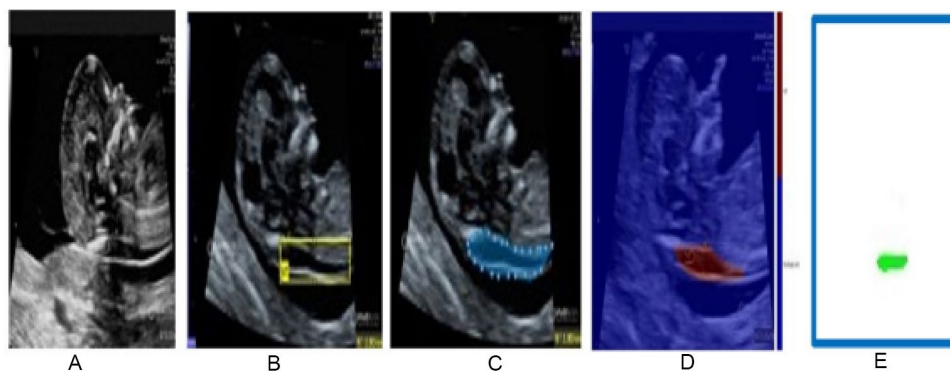


Fig. 3 Nuchal translucent in DS. Labeling explained. **a** speckle free image **b** selection of NT region **c** Manual labeling of an NT area using Pixel labeler **d** pixel labeled images **e** Final segmented output. Techniques for pre-processing, such as filtering and scaling,

are applied to the US photos. Filtering enhances the image quality, reduces noise, and preserves fine details at the edges. A Wiener filter is utilized to filter the image with improved results [7]

calculation. This involves initial Lee filter pre-processing, followed by manual extraction of the Region of Interest. The segmentation process is facilitated through morphological operations and Otsu thresholding. For a normally developing fetus, the typical nuchal translucency thickness is found to be 1.99 mm with a standard deviation of 0.62 mm. Additionally, the area is observed to be approximately 37.84 mm with a standard deviation of 20.28 mm, and the length measures around 126.44 mm with a standard deviation of 41.80 mm [2].

## Post natal

### Head and neck

In the head and neck, you can observe the following features: microcephaly (reduced head size), brachycephaly (brachycephaly without craniosynostosis), platybasia, and macroglossia. The ratio of biparietal diameter (BPD) to occipitofrontal diameter (OFD), which is known as the cephalic index (cephalic index =  $BPD/OFD \times 100$ ), increases and approaches the 95th percentile in cases of brachycephaly. This characteristic can be visually assessed and evaluated using neuroimaging studies. Figure 4 depicts the axial (a) and sagittal (b) T1/3D images of a 5-year-old Down syndrome child. Brachycephaly is a common feature, as evidenced by a higher cephalic index ( $129/147 \times 100 = 88$ ) compared to the normal range of 74–83, as determined by measurements of the biparietal and occipitofrontal diameters. The cranial sutures are still visible [3].

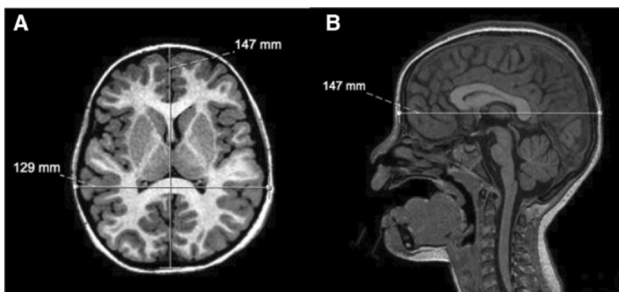


**Fig. 4** Brachycephaly in DS [3]

**Fig. 5** Platybasia in DS. Paranasal sinus reconstruction in the axial (c) and coronal (a, b) planes. A 21-year-old Down syndrome patient's CT scan showing hypoplasia of the maxillary and sphenoid sinuses and absent frontal sinuses [3]



When Down syndrome affects brain development, it results in a reduction in the size of the cerebellum, frontal cortex, and temporal cortex, along with a smoother appearance of the sulci and a narrower superior temporal gyrus [8]. Moreover, there are other recognized indicators of craniofacial morphology associated with Down syndrome, such as midface hypoplasia, malocclusion characterized by a posterior cross-bite and anterior open bite, advanced position of the tongue, and the presence of macroglossia. Additionally, Down syndrome is linked to a condition known as platybasia, which involves the flattening of the skull base and can be identified by an increase in the skull base angle. This angle is measured by a line connecting the nasion to the anterior border of the foramen magnum and the center of the pituitary fossa. Platybasia is defined as an angle exceeding 143 degrees (see Figs. 5 and 6) [3].

The reduction in brain size initially becomes apparent in fetuses at around 4–5 months of gestation, and it becomes more pronounced during the last trimester and postnatally. Brain MRI assessments conducted on individuals with Down syndrome (DS) of various ages have revealed a significant decrease in total brain volume when compared to age-matched controls, with a notable reduction of approximately 20%. The most substantial changes have been observed in the frontal lobes, hippocampi, and the brainstem, particularly the pons. Additionally, cerebellar and vermian hypoplasia are other noticeable features of this condition. Notably, the volume of deep gray matter structures remains within the normal range [3].

Furthermore, one of the most frequent CNS abnormalities associated with DS is the complete or partial agenesis of the corpus callosum. This condition can be caused by various factors, including prenatal infections, exposure to chemicals, vascular insults, and other genetic anomalies and disorders [3].

### Eye and ear

Visual issues in children with Down syndrome, such as substantial refractive errors, strabismus, nystagmus, and even cataracts, are more prevalent among them. Poor optical quality at a young age can affect the quality of the images processed by the retina and cortex. These children often



**Fig. 6** Platybasia in DS. A 38-year-old Down syndrome patient with platybasia (skull base angle  $> 143^\circ$ ) on sagittal T1/SE. This angle is calculated by drawing a line that connects the nasion with the center of the pituitary fossa and another line connecting the same point with the anterior border of the foramen magnum [3]

exhibit atypical visual abilities, including difficulties with visual acuity, low-contrast vision, vernier acuity, and accommodative acuity. The exact cause of this impaired visual performance associated with Down syndrome remains uncertain. Optical coherence tomography (OCT), a non-invasive imaging technique known for its high resolution, is gaining popularity for objectively and statistically evaluating the tissue structure of the fovea. The primary pathology in this condition may involve thicker macular structures (Fig. 7) [9].

In general, hearing loss is a common issue among individuals with Down syndrome, affecting between 38 and 78% of patients, indicating a relatively high prevalence. The most common inner ear abnormality in Down syndrome (DS) is the presence of a bony island in the lateral semi-circular canal (LSCC), defined as a measurement of 3 mm or less, with a prevalence of nearly 50%. This bone island can also undergo a transformation during embryological development, resembling a small bud known as the vestibular anlage (see Fig. 8). Semicircular canal dehiscence, with an approximate incidence of 9%, is another type of semi-circular canal defect often associated with DS [3].

In 75% of instances, children with Down syndrome experience sensorineural hearing loss (SNHL), which is typically detectable through computed tomography (CT) and/or magnetic resonance imaging (MRI) scans of the temporal bone. The most common inner ear anomaly in Down syndrome (DS) is the presence of a bony island in the lateral semi-circular canal (LSCC), defined as measuring 3 mm or less, with a prevalence of approximately 50%. During embryological

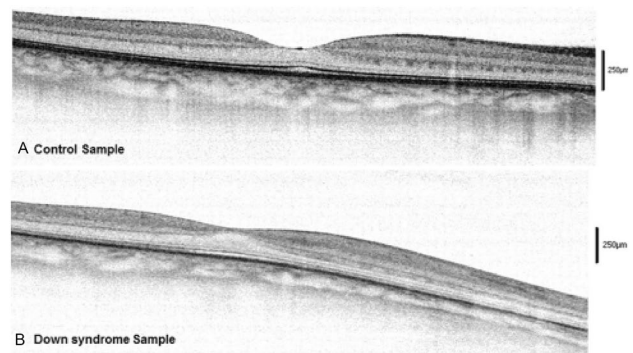


**Fig. 7** OCT images of healthy samples and DS samples. **a** An OCT image taken from a healthy, full-term 11-year-old child in the control group's right eye. The visual acuity was 20/20 at the time of testing, and the central subfield thickness (CST) of the entire retina is 235  $\mu$ m. This infant had a normal retina and a spherical equivalent of 0.75 D. The central thickness and foveal pit were both normal. **b** An OCT image taken from the right eye of a 13-year-old Down syndrome patient who was born at 38 weeks gestation. CST is 281  $\mu$ m, and the test subject's visual acuity was 20/65. In comparison to the control group, the patient's whole retina was substantially thicker and had a spherical equivalent of 1.5 D [9]

development, this bony island can also undergo complete regression, resembling a small bud similar to the vestibular anlage [3].

### Cardiovascular

Approximately 40–45% of individuals with Down syndrome typically have congenital heart diseases. Researchers have reported varying rates of occurrence for congenital heart conditions. These conditions include aortic coarctation, patent ductus arteriosus, tetralogy of Fallot, atrial septal defect,

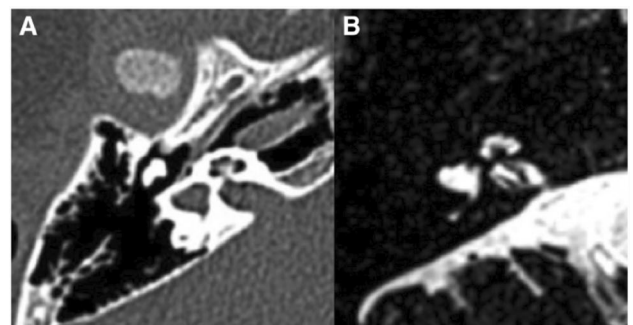


**Fig. 8** Inner ear anomaly in DS. A 2-year-old Down syndrome patient's temporal bone CT (**a**) and MRI (axial T2/3D) (**b**) at the level of the internal auditory canal, demonstrating total absence of the right bony island and aplasia of the lateral semi-circular canal as a result. It is important to observe the presence of a dysplastic vestibule due to the absence of the lateral semi-circular canal [3]

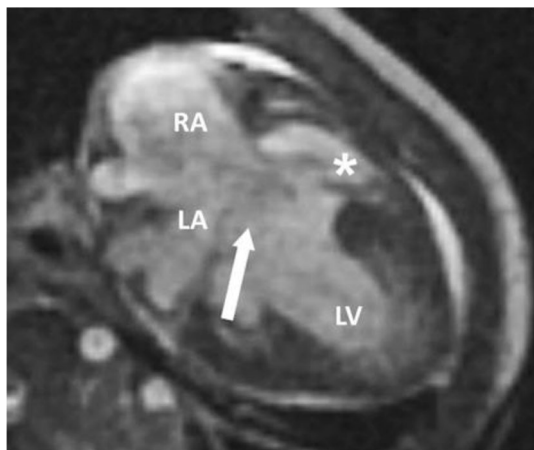


**Fig. 9** Atrioventricular defect in DS. An 11-week-old Down syndrome child's four-chamber image on a white-blood gradient echo cardiac MRI reveals a moderate to severely hypoplastic, non-forming right ventricle (\*), along with a left-ventricular dominant atrioventricular canal defect (arrow). LV left ventricle, LA left atrial, and RA right atrium [10]

and atrioventricular septal defect (AVSD), as illustrated in Fig. 9 [10].

In children diagnosed with tetralogy of Fallot, radiographs may reveal diminished pulmonary blood vessel markings and a distinctive boot-shaped heart. The abnormal shape of the heart is attributed to right ventricular hypertrophy and a narrow mediastinum resulting from underdeveloped pulmonary arteries, although these features may not always be present. Cardiac CT and MR imaging are commonly used, especially in adolescent and adult patients, to assess the heart between staged operations or after surgery [10].

### Respiratory system

Respiratory problems are the leading cause of increased mortality in children with Down syndrome, along with being the primary reason for hospital admissions. Pneumonia, the most common respiratory ailment in this group, accounts for nearly 80% of hospitalizations and admissions to intensive care units for these children [10].

Children with Down syndrome who have RSV bronchiolitis exhibit similar radiographic findings to other children, including hyperinflated lungs, streaky parahilar opacities, and bronchial cuffing in radiographs. However, a notable difference is that children with Down syndrome are more prone to radiographic consolidation, as illustrated in Fig. 10 [10].

Obstructive sleep apnea is the second most common respiratory condition in children with Down syndrome, affecting 30–75% of them. Lateral airway radiographs can reveal relative macroglossia, along with a narrowing of the nasopharyngeal and oropharyngeal airways due to the enlargement of the adenoids, soft palate, palatine, and



**Fig. 10** Respiratory syncytial virus bronchitis in DS. A 14-month-old girl with Down syndrome has symmetrical hyperinflation of the lungs, streaky perihilar opacities, and various isolated right upper lobe opacities shown on an anterior–posterior radiograph of the chest. The girl was identified as having RSV bronchiolitis, or respiratory syncytial virus [10]

lingual tonsils. To assess the functionality of these children's upper airways, dynamic cine MRI can be employed. Common findings include recurring and enlarged adenoids, glossoptosis, hypopharyngeal collapse, increased lingual tonsils, and macroglossia [10].

### Gastrointestinal tract

Most areas of the gastrointestinal system may be affected by congenital gastrointestinal abnormalities, which affect four to ten percent of children with Down syndrome. Duodenal atresia, which affects one to five percent of people with Down syndrome, is the most frequent gastrointestinal aberration. Down syndrome affects 30% of newborns with duodenal atresia [10].

A characteristic double-bubble look with an inflated, fluid-filled stomach and proximal duodenum can be seen on fetal sonography or MRI. Polyhydramnios is frequently found. A postnatal radiograph reveals a double bubble filled with air and no distal intestinal gas (Fig. 11) [10].

Annular pancreas is more common in children with Down syndrome. One study indicated that the risk of annular pancreas is 430 times higher in children with Down syndrome compared to those without the syndrome. On radiographs, annular pancreas can sometimes mimic a double bubble, but there is typically gas present in the distal small bowel, unlike the characteristic findings of duodenal atresia. Fluoroscopy reveals a circular constriction in the second part of the duodenum. During endoscopic retrograde cholangiopancreatography, the pancreatic duct encircles the duodenum,

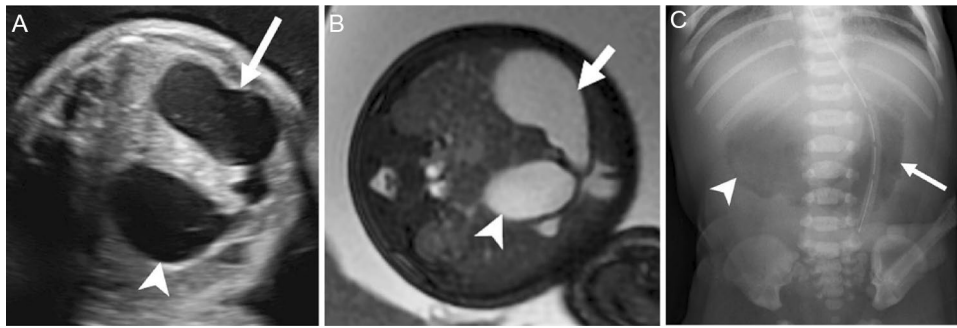


**Fig. 11** Duodenal atresia in DS. A 33-week-old fetus with Down syndrome may be seen in **a** a prenatal ultrasonography and **b** a prenatal FIESTA (fast imaging exploiting steady-state acquisition) MR image with a dilated stomach (arrow) and proximal duodenum (arrowhead), which are typical of the double-bubble sign of duodenal atresia.

There was polyhydramnios (not indicated). With a dilated stomach (arrow) and proximal duodenum (arrowhead), an abdominal radiograph of a different newborn with Down syndrome similarly exhibits the double-bubble look [10]

and cross-sectional imaging shows the pancreatic tissue surrounding the second part of the duodenum. Oral contrast agents can be used to help identify the duodenum in CT images [10].

Esophageal atresia with tracheoesophageal fistula is more common in Down syndrome compared to the general population, with a frequency of 0.3–0.8%. Children typically present with feeding difficulties and increased oral secretions. Chest radiographs reveal a dilated, air-filled esophageal pouch. If an enteric tube is placed, it is often coiled within the esophageal pouch (as shown in Fig. 12). The presence of air in the stomach confirms the existence of a tracheoesophageal fistula (as shown in Fig. 12). Additional imaging is seldom necessary to confirm the diagnosis of esophageal atresia [10].

One of the most frequently observed midgut abnormalities in individuals with Down syndrome is malrotation, with a reported incidence approximately 45 times higher compared to children without Down syndrome. Children afflicted with malrotation and midgut volvulus typically exhibit bilious vomiting during the first week after birth. Abdominal radiographs may appear normal or indicate signs of a proximal blockage. The next diagnostic step usually involves an upper gastrointestinal study, which reveals an abnormal positioning of the duodenojejunal junction, where the duodenum remains to the right of the spine and descends inferiorly (Fig. 13) [10, 11].

The most frequently observed lower digestive tract issues in children with Down syndrome include constipation, Hirschsprung disease, and anorectal malformations.

Hirschsprung disease (HD) is a type of lower intestinal blockage that results from the absence of normal myenteric ganglion cells in a specific segment of the colon. This condition represents roughly 15–20% of cases of neonatal bowel obstruction. Approximately 2% of individuals with Hirschsprung disease also have Down syndrome. The

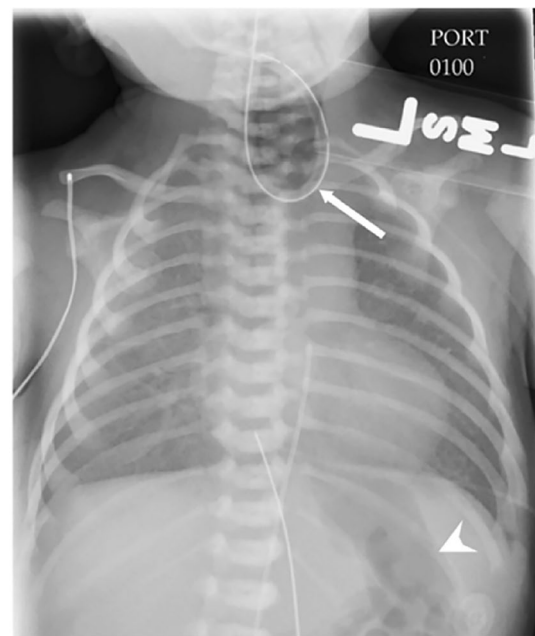


**Fig. 12** Tetralogy of Fallot and esophageal atresia/tracheoesophageal fistula. Anteroposterior chest radiograph in a newborn boy shows that the heart has a boot-shaped contour with an upturned apex compatible with a diagnosis of tetralogy of Fallot. A nasoenteric tube is coiled in the upper esophageal pouch (arrow), consistent with esophageal atresia. The presence of bowel gas (arrowhead) in the upper abdomen confirms the presence of a tracheoesophageal fistula

affected segment lacking ganglion cells varies in length but consistently extends upwards from the anal canal, with the rectosigmoid region being involved in 80% of cases [10, 12].

Radiographic examinations in children with HD reveal findings that resemble those in other forms of lower small bowel obstruction, including variable gaseous distention of the colon and small bowel, often accompanied by air–fluid levels. Contrast enema is a valuable tool for investigating

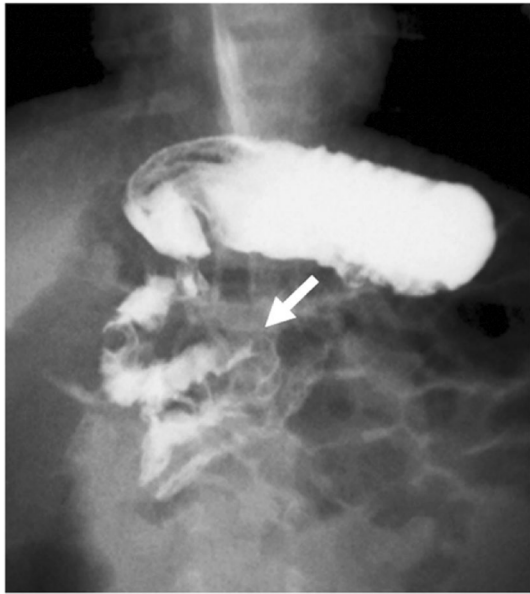


**Fig. 13** Malrotation in DS. Anteroposterior image in a 5-month-old girl with Down syndrome who presented with emesis shows an abnormal position of the duodenojejunal junction (arrow), which is positioned closer to midline and lower than the pylorus, indicating malrotation

distal bowel obstruction in neonates. The most characteristic radiological finding in HD is the presence of a transition zone between the narrowed and dilated sections of the colon, resembling an inverted cone on a barium enema study. However, the bowel distention above the under innervated segment occurs gradually, and a transition zone is observed in only 50% of neonates during the first week of life. Other findings noted in barium enema studies include a rectosigmoid ratio of less than 1, a sawtooth appearance of the denervated colon due to muscle spasms, an irregular or thickened colon wall associated with colitis, and a delay in the evacuation of contrast material, which can take more than 24–48 h. A definitive diagnosis necessitates a rectal biopsy (Fig. 14) [10].

Another congenital gastrointestinal abnormalities that can be found during antenatal ultrasound examination is imperforate anus. Imperforate anus is caused by hindgut development defect during pregnancy. Imperforate anus is not a life-threatening anomaly but it is related to chromosomal anomalies. Imperforate anus appears as an hypoechoic ring with an echogenic center in ultrasound (Fig. 15) [13].

### Abdominal parenchymal organs

Recently, studies have shown that hypoechoic liver can be a soft marker for DS. A retrospective analysis result had shown that 55.5% cases of proven DS had hypoechoic liver. Hypoechoic liver is defined as liver echogenicity was less

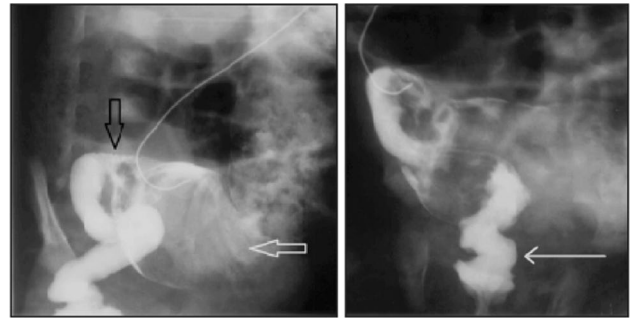


**Fig. 14** Serial images from a contrast enema study show the presence of a transition point (black open arrow) between the narrowed and dilated portions (white open arrow) of the colon, at the mid sigmoid colon. Mild fasciculations from spasm is seen within the rectum (white arrow). A short segment Hirschsprung's disease was confirmed at rectal biopsy

than that of the adjacent lung and bowel with conspicuous visualization of diaphragm (Fig. 16) [14, 15].

Pancreas abnormalities can be found DS. Prenatal diagnosis of annular pancreas is very rare but it is associated with other abnormalities including DS. Annular pancreas is the third most common gastrointestinal abnormalities found in patients with DS.

### Musculoskeletal system

In a previous cohort study, pes planus, characterized by the loss of the medial longitudinal arch in the feet, was found in nearly all cases (91%). Among these children, however, a quarter (24%) did not utilize orthotic devices [16]. Additionally, the first metatarsal web space, often referred to as the "sandal gap sign," frequently widens in the feet. This characteristic is observed in 45% of children with Down syndrome, though it is not exclusive to this condition (see Fig. 17). An anteroposterior radiograph of a 5-day-old child with Down syndrome's foot shows an enlarged first

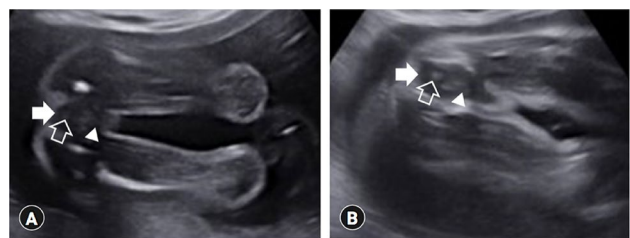


**Fig. 15** Fetal Ultrasound **A** At 30 weeks of gestation, an echogenic ring is seen (open arrow) in the hypoechoic area (solid arrow) suggesting an intact anus with a short perineal body (arrowhead). **B** At 35 weeks of gestation, a short perineal body (arrowhead) is revealed, an echogenic ring (open arrow) indicating the anal mucosa in hypoechoic area (solid arrow) is seen





**Fig. 16** Hypochoic liver with prominent ductal walls and vascular



**Fig. 17** Sandal gap sign

intermetatarsal space (indicated by the arrow), which is sometimes referred to as the sandal gap sign [10].

In children with DS, we can find atlantoaxial instability (AAI). AAI is more common in children with DS resulting from ligament laxity and odontoid dysplasia. Atlantoaxial dislocation is Atlantoaxial dislocation is defined by a loss of stability between the atlas and the axis (C1–C2), which results in a loss of standard articulation. Children with down syndrome also have low mineral density, low muscle tone, and excessive joint flexibility (Fig. 18) [17].

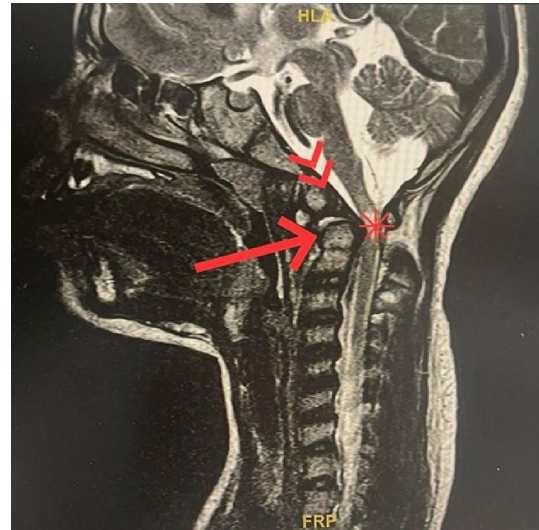


**Fig. 18** Atlantoaxial subluxation with subsequent compressive myelopathy at the C1 level (Normal variant of os odontoideum (double arrow) superimposed with retroverted odontoid process (arrow), focal compression of the upper cervical cord and subsequent chronic myelopathy (asterisk))

### Genitourinary system

Pyelectasis, also known as renal dilatation or hydronephrosis, is a common finding on fetal ultrasound. Pyelectasis is detected by measuring anteroposterior renal pelvic diameter (APRPD). Recently, there is no consensus about the threshold of APRPD. Early second trimester pyelectasis can be a marker for DS. Isolated renal pyelectasis during second trimester of pregnancy increased risk by 2.78 for DS. It is important to note that pyelectasis finding also found in fetal with or without urinary tract abnormalities and resolved spontaneously during pregnancy. This finding should be taken into account; also genetic counseling and testing should be conducted to rule out DS (Fig. 19) [18].

Although less commonly encountered, renal and urinary tract abnormalities manifest in 3.2% of children with Down syndrome, a prevalence nearly five times higher than that in the general population. The predominant observation is urinary obstruction, characterized by varying degrees of hydronephrosis and hydroureter. This obstruction may manifest at different levels, including the urethra, ureterovesical junction, or ureteropelvic junction. The incidence of posterior urethral valves in children with Down syndrome exceeds that in the general population [10].

Additional associated urinary anomalies encompass megaureter, vesicoureteral reflux, hypospadias, renal agenesis, renal dysplasia, horseshoe kidney, and glomerular microcysts. Beyond congenital urinary tract anomalies, children with Down syndrome face an elevated risk

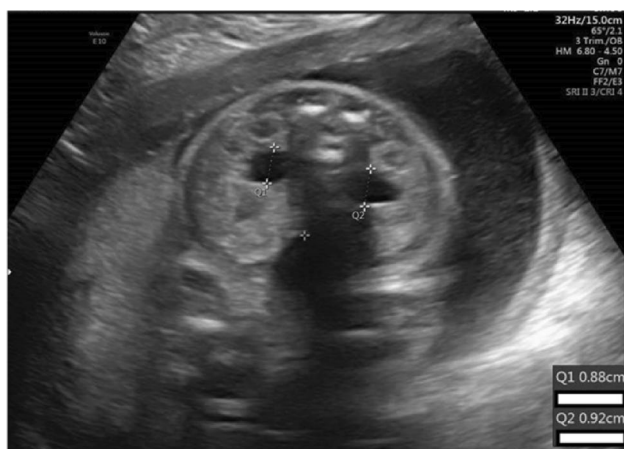


**Fig. 19** Bilateral pyelectasis at second trimester (24 weeks of pregnancy)

of medical renal diseases, including glomerulopathies. As these conditions are potentially correctable, there is a strong advocacy for early screening to identify anatomical renal and urological abnormalities in infants with Down syndrome [10].

## Conclusions

Down syndrome is associated with various radiological features. Indicators of Down syndrome can include the presence of atrioventricular septal abnormalities, tetralogy of Fallot, macroglossia, esophageal atresia, microcephaly, and structural alterations in the musculoskeletal system. During fetal imaging, it is important to assess the volume of amniotic fluid, particularly in the context of nuchal translucency, as well as determine the presence or absence of nasal bones in the fetus.

**Author contributions** JJW supplied and gathered the literature for the review. CF, MGW, JL and RS reviewed the material and contributed significantly to the creation of the paper.

**Funding** All resources provided by the authors.

**Availability of data and materials** Data sharing is not applicable to this article as no datasets were generated or analyzed during the current study.

## Declarations

**Conflict of interest** The authors declare that they have no competing interests.

**Ethical approval and consent to participate** Not applicable.

**Consent for publication** Not applicable.

## References

- García-García MT, Diz-Dios P, Abeleira-Pazos MT, et al. Cranial-Vertebral-maxillary morphological integration in Down syndrome. *Biology (Basel)*. 2022. <https://doi.org/10.3390/biology11040496>.
- Shiney J, Singh OJAP, Shan BP. A review on techniques for computer aided diagnosis of soft markers for detection of Down syndrome in ultrasound fetal images. *Biomed Pharmacol J*. 2017;10:1559–68.
- Rodrigues M, Nunes J, Figueiredo S, et al. Neuroimaging assessment in Down syndrome: a pictorial review. *Insights Imaging*. 2019;10:52.
- Manohar J. The assessment of nasal bone during gestation to screen for down syndrome: a review. *J Pharm Sci Res*. 2016;8:607–12.
- Pranpanus S, Keatkongkaew K, Suksai M. Utility of fetal facial markers on a second trimester genetic sonogram in screening for Down syndrome in a high-risk Thai population. *BMC Pregnancy Childbirth*. 2022;22:27.
- Van Keirsbilck J, Dewulf V, Van Calsteren K, et al. Comparison and reproducibility of nuchal translucency measurements using two-dimensional and volume nuchal translucency ultrasound: a prospective study. *Fetal Diagn Ther*. 2013;34:103–9.
- Thomas MC, Arjunan SP. Deep learning measurement model to segment the nuchal translucency region for the early identification of Down syndrome. *Meas Sci Rev*. 2022;22:187–92.
- Lao PJ, Handen BL, Betthausen TJ, et al. Imaging neurodegeneration in Down syndrome: brain templates for amyloid burden and tissue segmentation. *Brain Imaging Behav*. 2019;13:345–53.
- O'Brien S, Wang J, Smith HA, et al. Macular structural characteristics in children with Down syndrome. *Graefes Arch Clin Exp Ophthalmol*. 2015;253:2317–23.
- Radhakrishnan R, Towbin AJ. Imaging findings in Down syndrome. *Pediatr Radiol*. 2014;44:506–21.
- Sk P, Kandasamy D, Jana M, et al. Pediatric stomach and duodenal imaging. *J Gastrointest Abdom Radiol*. 2021;04:094–108.
- Amiel J, Sproat-Emison E, Garcia-Barcelo M, et al. Hirschsprung disease, associated syndromes and genetics: a review. *J Med Genet*. 2007;45:1–14.
- Kim HM, Cha H-H, Kim JI, et al. The diagnosis of an imperforate anus in female fetuses. *Yeungnam Univ J Med*. 2021;38:240–4.
- Balusamy S, Rajee AM, Radhakrishnan S, et al. Hypochoic liver: a promising soft marker in screening for Trisomy 21. *Ultrasound Obstet Gyne*. 2022;60(S1):137–8.
- Omar PM, Lim WT, Ting YH, et al. Hypochoic liver in fetuses with trisomy 21. *J Matern Fetal Neonatal Med*. 2019;32:3315–7.
- Foley C, Killeen OG. Musculoskeletal anomalies in children with Down syndrome: an observational study. *Arch Dis Child*. 2019;104:482–7.
- Alfhami S, Sejeeni N, Alharbi K, et al. Atlantoaxial subluxation in a 10-year-old girl with Down syndrome: a case report. *Cureus*. 2023. <https://doi.org/10.7759/cureus.43955>.
- Farladansky-Gershnel S, Gluska H, Meyer S, et al. Postnatal outcomes of fetuses with prenatal diagnosis of 6–9 mm pyelectasis. *Children*. 2023;10:407.

**Publisher's Note** Springer Nature remains neutral with regard to jurisdictional claims in published maps and institutional affiliations.

Springer Nature or its licensor (e.g. a society or other partner) holds exclusive rights to this article under a publishing agreement with the author(s) or other rightsholder(s); author self-archiving of the accepted manuscript version of this article is solely governed by the terms of such publishing agreement and applicable law.